DOPPLER ORBIT DETERMINATION OF DEEP SPACE PROBES BY THE BERNESE GNSS SOFTWARE: FIRST RESULTS OF THE COMBINED ORBIT DETERMINATION WITH INTER-SATELLITE KA-BAND DATA FROM THE GRAIL MISSION

Stefano Bertone(1), **Adrian Jäggi**(2), **Daniel Arnold**(3), **Gerhard Beutler**(4), **and Leos Mervart**(5)

(1)(2)(3)(4)*Astronomical Institute, University of Bern, Sidlerstrasse 5, 3012 Bern, e-mail: stefano.bertone@aiub.unibe.ch*

(5)*Institute of Advanced Geodesy, Czech Technical University, Thakurova 7, 16629 Prague 6-Dejvice, Czech Republic*

Abstract: *Navigation of deep space probes is most commonly operated using the spacecraft Doppler tracking technique. Orbital parameters are determined from a series of repeated measurements of the frequency shift of a microwave carrier over a given integration time. Currently, both ESA and NASA operate antennas at several sites around the world to ensure the tracking of deep space probes. Just a small number of software packages are nowadays used to process Doppler observations. The Astronomical Institute of the University of Bern (AIUB) has recently started the development of Doppler data processing capabilities within the Bernese GNSS Software. This software has been extensively used for Precise Orbit Determination of Earth orbiting satellites using GPS data collected by on-board receivers and for subsequent determination of the Earth gravity field. In this paper, we present the currently achieved status of the Doppler data modeling and orbit determination capabilities in the Bernese GNSS Software using GRAIL data. In particular we will focus on the implemented orbit determination procedure used for the combined analysis of Doppler and intersatellite Ka-band data. We show that even at this earlier stage of the development we can achieve an accuracy of few mHz on two-way S-band Doppler observation and of* 2 *μm/s on KBRR data from the GRAIL primary mission phase.*

Keywords: *orbit determination, Doppler, Bernese GNSS Software, GRAIL*

1. Introduction

In modern times, the most common navigation technique of deep space probes is the spacecraft Doppler tracking technique. Orbital parameters are determined from a series of repeated measurements of the frequency shift of a microwave carrier over a given integration time. Currently, both ESA and NASA operate antennas on several sites around the world to ensure the tracking of deep space probes using S-band , X-band and K-band one-way, two-way and three-way radio links. Doppler measurements are also commonly used in planetary geodesy, where the spacecraft orbit is used as basis for the determination of the gravity field coefficients. Only a handful of software packages are nowadays used to process deep space Doppler observations, e.g. GEODYN (NASA GSFC, [1]), MIRAGE/MONTE (NASA JPL, [2]), GINS (CNES, [3]) and ESOC's Orbit Determination System (ESA, [4]). The Astronomical Institute of the University of Bern (AIUB) has recently started the development of Doppler data processing capabilities within the Bernese GNSS Software [5]. This software has been extensively used for Precise Orbit Determination (POD) of Earth orbiting satellites using GPS data collected by on-board receivers and for subsequent determination of the Earth gravity field. Based on the GRACE [6] processing chain established at AIUB, procedures have been extended to also perform orbit and gravity field determination from data collected by the NASA mission GRAIL (Gravity Recovery And Interior Laboratory) as illustrated in [7]. This mission uses both Doppler tracking from Earth and ultra-precise inter-satellite Ka-band range-rate (KBRR) observations, which has enabled for the first time high-quality data acquisition also on the entire far-side of the Moon [8]. This data allows for a highly accurate lunar gravity field determination, as demonstrated by the spectacular high resolution solutions computed at NASA GSFC and NASA JPL (see, e.g., [9, 10]). In this paper, we present the currently achieved status of the Doppler data modeling and orbit determination capabilities in the Bernese GNSS Software using GRAIL data. In particular we will focus on the implemented orbit determination procedure used for the combined analysis of Doppler and intersatellite Ka-band data. Despite the heritage from GRACE, there are major differences, e.g., due to the inhomogeneous tracking of the GRAIL orbits by ground stations tracking. First, we will solve a classical orbit determination problem for each GRAIL satellite separately by using only Doppler data. The orbits will be parametrized by initial osculating orbital elements and a small number of empirical orbit parameters to handle remaining model deficiencies. The orbits emerging from this procedure will then serve as a priori orbits for the subsequent KBRR analysis. Using the outlined procedure, we identify optimal weighting and empirical orbit parametrization when using gravity field models of different quality, e.g., the solutions emerging from the GRAIL mission and from the pre-GRAIL era. We analyze the quality of our computed orbits against the GNI1B positions provided on the Planetary Data System (PDS, [17]) servers and resulting from the NASA JPL orbit and gravity field determination. Moreover, we often refer to the orbit components in the orbital frame as radial (R), along-track (A) and out-of-plane (O).

This paper is structured as follows. In Section 2. we provide some generalities about Doppler orbit determination, while in Section 3. we detail our approach for a combined Doppler and KBRR procedure for GRAIL. We then provide our results in GRAIL data processing and orbit determination in Section 4.. We conclude with our considerations and an outlook on future developments of this study in Section 5..

2. Doppler orbit determination

Deep space navigation is based on the exchange of radio signals between a probe and at least one observing ground station. Based on the propagation time of the exchanged signals, two kinds of observables are produced: the ranging and the Doppler. Ranging is related to the distance between the emitter and the receiver, while Doppler is related to the radial velocity along the line of sight. Several configurations are possible :

- the one-way link, when the probe emits a downlink signal towards a tracking ground station;
- the two-way link, when a ground station emits an uplink signal towards the probe, which copies it to re-emit a downlink signal towards the same ground station;
- the three-way link, when the receiving station is different from the emitting one.

Several frequencies are used for the exchanged signals, especially in the S-band ($2 - 4$ GHz), X-band ($7 - 11$ GHz) and recently in the K-band ($26.5 - 40$ GHz) to further improve accuracy.

In order to be able to perform orbit determination (OD) for deep-space probes, we recently implemented Doppler capabilities in the Bernese GNSS Software. In particular, we invested in an accurate modeling of light propagation in deep space including first order relativistic effects and atmospheric delay. The formulation of the one-way and two-way Doppler observables implemented in the Bernese GNSS Software follows the guidelines given in [2] as well as the latest IERS [11] and IAU conventions [12]. Doppler observations are eventually accumulated over the chosen integration time and screened for outliers by using a simple threshold criteria.

3. Combined Doppler and KBRR orbit determination for GRAIL

We use the Doppler observations together with the ultra-precise KBRR observations for a combined orbit determination of GRAIL probes. The background framework and force model includes contributions from the gravity potential of the Moon, the third-body accelerations from other Solar System bodies, accelerations due to the tidal deformation of the Moon and relativistic corrections. We currently do not explicitly model non-gravitational accelerations (e.g., solar radiation pressure), which are accounted for by empirical accelerations and pseudo-stochastic pulses [13].

Following a procedure similar to [14], we perform the following steps:

- Set up of two normal equation systems based on GRAIL-A and GRAIL-B Doppler observations as part of a reduced-dynamic OD procedure [15]. We set up six initial osculating elements and eventually empirical accelerations in all directions (estimated once per arc) and pseudo-stochastic pulses acting in the same directions.
- Set up of one normal equation system based on KBRR observations using the same orbit parametrization. In addition to the parameters specified in the first step, specific Ka-band parameters may be set up. Due to the presence of the orbit parameters of both satellites, the normal equations set up in this step are singular when used alone.
- The three normal equation systems are combined by setting up an appropriate weighting ratio, e.g., based on the relative accuracy of the observations. In the case of Doppler S-band observations and KBRR data, we can assume a relative weighting of $1 : 10^8$ [7].

4. Results in the context of the GRAIL mission

We applied the methodology described in Section 3. to the GRAIL mission. In our analysis, we consider two different cases:

1. the case of a background field derived from the GRAIL mission, in particular we will use GRGM900C [10] truncated to d/o 300;
2. the case of using a pre-GRAIL field as background field, in particular the SELENE derived lunar gravity field SGM150J [16].

We focus the processing on two-way Doppler data from the primary mission (PM) phase publicly available on the PDS servers. Indeed, the processing of one-way data from the GRAIL mission requires additional screening of the data and the estimate of dedicated parameters, especially because of the disruption of the onboard clock following a solar flare on the first days of the mission [18].

In the context of planetary missions, Doppler orbit determination is a complex matter since radio communications with the probe are only possible when the latter is visible from the Earth. For this reason and because of the limited availability of tracking time for each spacecraft, Doppler observations are available only for several hours per day. We can consider two "extreme" geometries for observations taking place in the Earth-Moon system and repeating every two weeks over the three months of the PM phase:

- the "face-on" geometry, when the orbital plane is perpendicular to the line of sight. In this particular configuration, the full orbit of the probe around the Moon is visible from Earth. However, the radial velocity of the probe w.r.t. the observer is close to 0, so that orbit determination is very difficult. As soon as we slightly move away from this "extreme" scenario, anyway, the situation is favorable;
- the "edge-on" geometry, when the orbital plane is parallel to the line of sight. A large portion of the orbit is then not visible from Earth. The along-track component of the orbit is well constrained by observations, while the cross-track component is difficult to determine. In this paper, we often highlight observation times in this geometry by a gray shading.

4.1. Doppler-only orbit determination

We process two-way Doppler observations provided by several stations of the Deep Space Network (DSN), distributed over three sites (Goldstone, Canberra and Madrid). The data is first accumulated to an integration time of 10 s (from 1 s observations provided on the PDS), then screened by applying a threshold of 20 mHz to the differences between Doppler measurements and observations simulated using the GNI1B positions. The resulting observations are fitted in one-day arcs in the orbit determination process. In the following, we detail our orbit parametrization and results for the two cases illustrated in 4.. We will focus on GRAIL-A but similar results also apply to GRAIL-B.

Fig. 1 shows the two-way Doppler residuals for GRAIL-A obtained adopting different parametrizations and GRGM900C used up to d/o 300 as background gravity field. It also shows orbit differences w.r.t. GNI1B positions: a bias is present in the resulting A component of the orbit, while the determination of the O component is difficult especially in edge-on geometry. The fit of a purely dynamic orbit to the data provides Doppler residuals with an average RMS of 7 mHz over the PM phase, as illustrated in Figure 2. A large two-weekly signal due to different observation geometries with respect to the Earth is present. Also, a once-per-revolution (opr) signal with an amplitude of up to 20 mHz is clearly visible in Fig. 1.

We noted that estimating empirical accelerations and pulses in all directions could worsen our orbits (even though Doppler residuals improved). Moreover, the effect of accelerations in R and A directions on the orbit is quite similar.

We also analyzed the optimal spacing between pulses with different constraints on their amplitude. As for empirical accelerations, pulses in R and A directions have similar effects on the resulting orbit and we finally identified an optimal parametrization consisting in:

- a constant acceleration in A and a opr acceleration in R direction, estimated once per arc;
- regularly spaced pulses every 30' in A and O directions, both constrained to zero.

Fig. 1 shows how this parametrization helps improving the Doppler residuals when comparing with the purely dynamic orbit. Biases and once per revolution signals in the orbit differences w.r.t. the GNI1B positions are also significantly reduced.

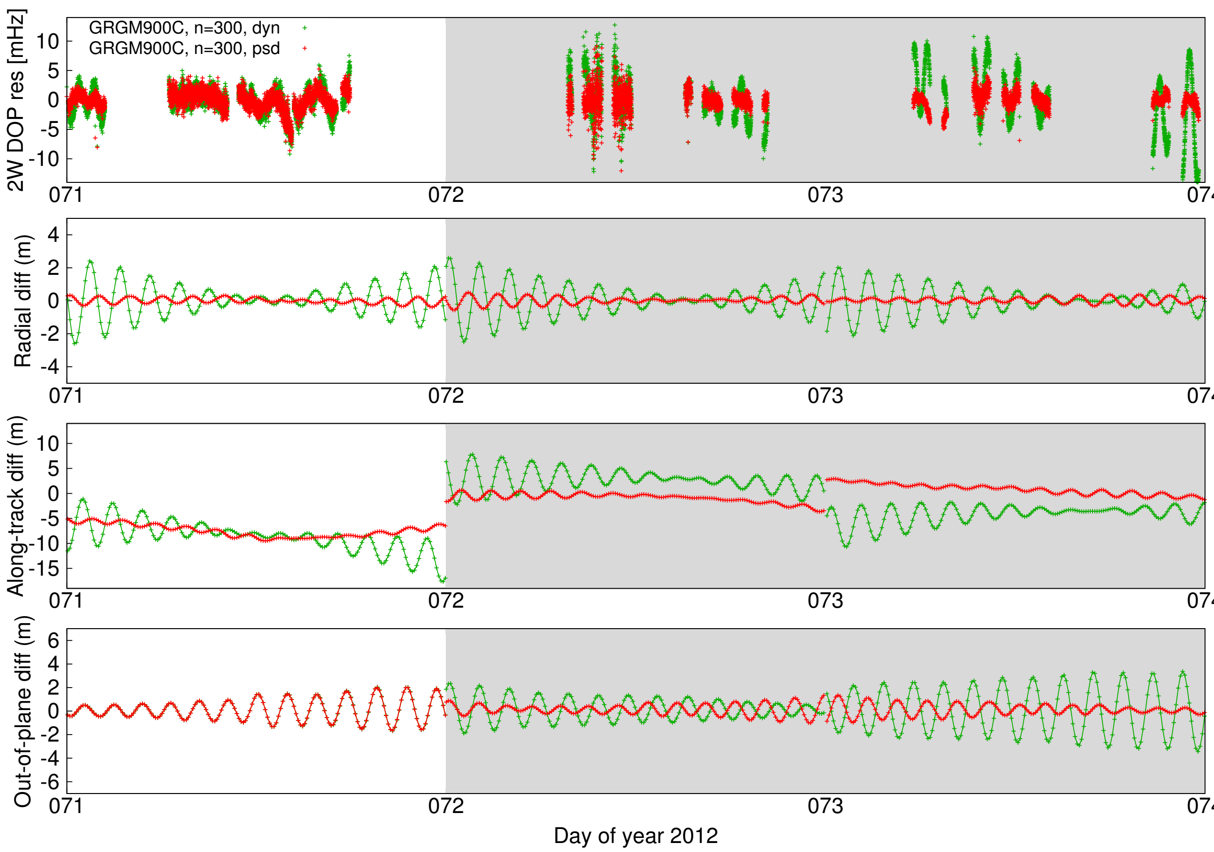

Figure 1. On the top: Two-way Doppler residuals for an integration time of 10 s on days 071-073 of 2012. Below, orbit differences w.r.t. GNI1B positions in R, A, and O directions). We use GRGM900C truncated at d/o 300 as background gravity field and different parametrizations: ”dyn” indicates a purely dynamic orbit, while for ”psd” we have estimated additional constant accelerations in A and opr accelerations in R as well as pulses in A and O directions every 30’. The shaded areas show the intervals of observations in edge-on geometry.

In order to highlight the difficulties of performing Doppler based orbit determination using a ”poorer” gravity field (as generally available in planetary probes navigation), we use the SELENE field SGM150J to estimate a dynamic orbit for GRAIL probes. As shown in Fig. 2, the resulting Doppler residuals and position differences are significantly worse.

Moreover, the use of equally spaced pulses for such a poorly constrained problem (due to the discontinuities in the Doppler observations) is particularly delicate when working with pre-GRAIL lunar gravity fields. We performed some preliminary experiments by relating the constraint applied on the pulses to the presence of a minimum number of observations in the considered interval. However, at this early stage, we stick to a purely dynamic orbit determination for this specific case.

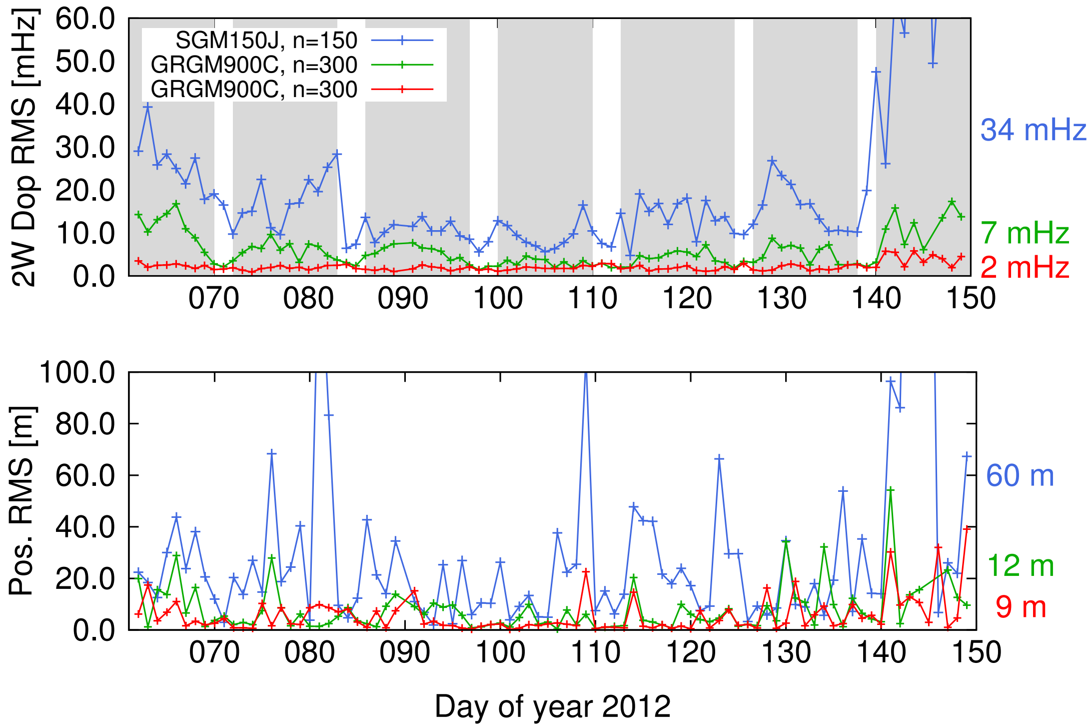

Figure 2. Daily RMS values of the Doppler residuals (top) and position differences (bottom, w.r.t. GNI1B) for GRAIL-A over the entire PM phase. The green curve corresponds to the purely dynamic orbit solution while the red one corresponds to the "optimal" parametrization described in the text. The numbers at the right-hand side are the mean RMS values. The shaded areas show the intervals of observations in edge-on geometry.

4.2. Impact of KBRR data on the relative positioning

The parametrizations selected in Section 4.1. are then applied in the combined orbit improvement with KBRR data. This is continuous, equally spaced and very accurate data providing informations about the relative velocity of the two spacecraft along the line of sight. This data hence provide an additional constraint to our orbit determination problem, in particular regarding the along-track component of the orbit.

We then used the improved orbits for both GRAIL-A and GRAIL-B to compute KBRR residuals in case 1 and 2. We note that KBRR residuals based on SGM150J are at least one order of magnitude larger than those computed using GRGM900C. The relation between residuals amplitude and geometry of the observations is also clearly visible in this case (see Fig. 4). On the other hand, when using GRGM900C (up to d/o 300) as background field and with the chosen parametrization we obtain KBRR residuals of 4.8 μm/s, only one order of magnitude larger than the nominal accuracy of the data. We get an even lower average RMS (1.7 μm/s) when not considering days 140 – 150 of 2012, when the probes where lower and a more accurate gravity field is definitely required. At this level, the missing non-gravitational forces modeling is a limiting factor.

A few days (2012 - 65, 90, 102) have to be screened out because of issues in the KBRR data.

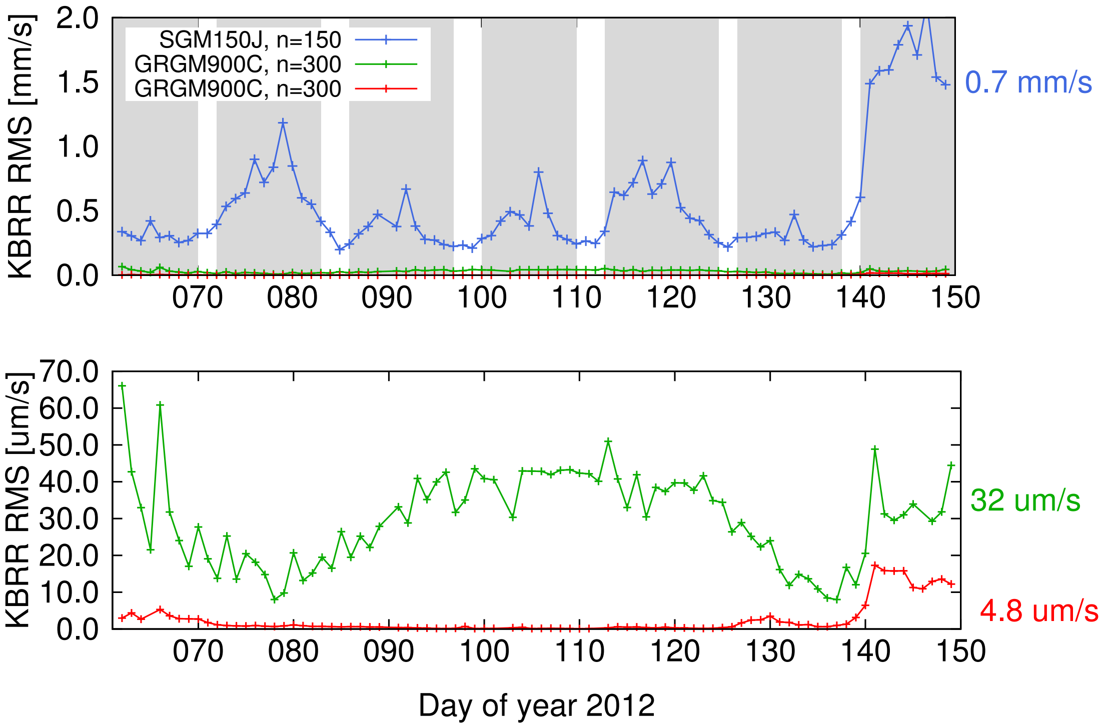

Figure 3. Daily RMS values of KBRR residuals over the entire PM phase for different background gravity fields and parametrizations. The numbers at the right-hand side are the average RMS values. The green curve corresponds to the purely dynamic orbit solution while the red one corresponds to the ”optimal” parametrization described in the text. The shaded areas show the intervals of observations in edge-on geometry.

4.3. Impact of KBRR data on the absolute orbit

Finally, we analyze the impact of KBRR data on the absolute orbits of the two satellites. As in previous sections, we compare our results to the GNI1B orbits in both cases 1 and 2 for GRAIL-A. Similar results also apply to GRAIL-B.

We observe in Fig. 4 a clear improvement for the orbit computed using GRGM900C (up to d/o 300) and the optimal parametrization. The global RMS is reduced to 2 m (less than 1 m when not considering days 140-150 of 2012). More in detail, we observe large improvements in A and O components. On the other hand, the orbits are worsened in the case of purely dynamic orbits or when using a ”poorer” gravity field. Experiments with different weightings of Doppler and KBRR data did not help to improve our results in this case.

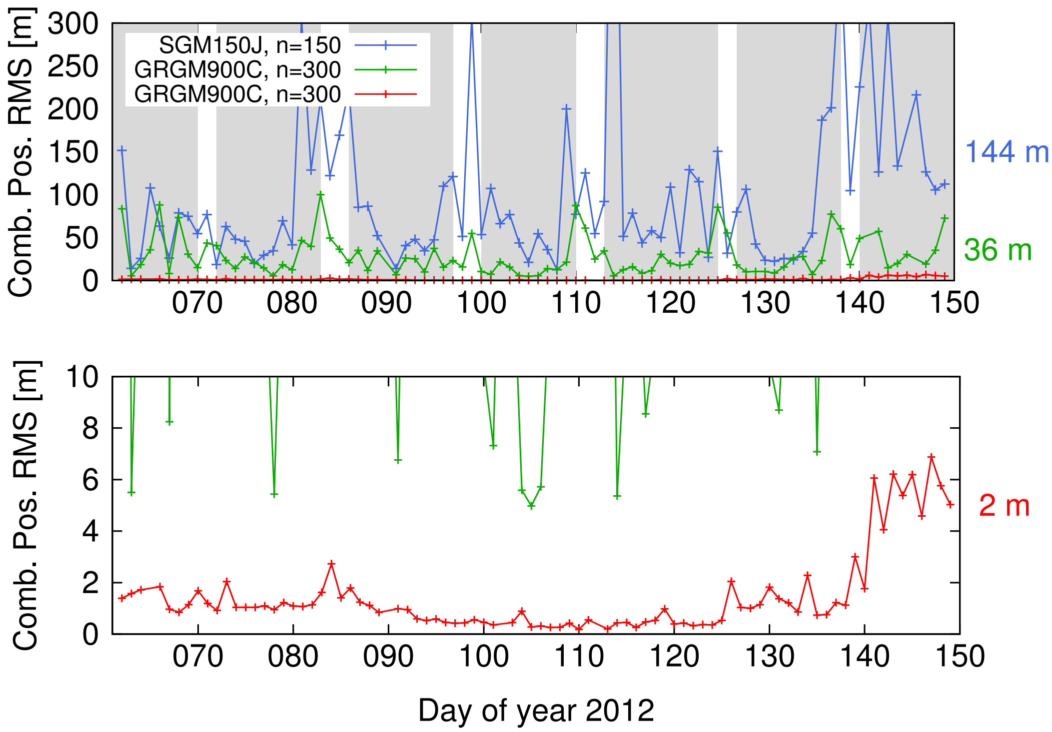

Figure 4. Daily RMS values of the position differences (w.r.t. GNI1B positions) over the entire PM phase. The numbers at the right-hand side are the average RMS values. The green curve corresponds to the purely dynamic orbit solution while the red one corresponds to the ”optimal” parametrization described in the text. The shaded areas show the intervals of observations in edge-on geometry.

5. Conclusions

Orbit determination capabilities from Doppler deep-space tracking have been recently developed in the framework of the Bernese GNSS software following the guidelines of [2] and the most recent conventions for Earth orientation. We present our first results about orbit determination of the GRAIL probes around the Moon from two-way Doppler observations and combined Doppler and KBRR data. In this context, we show our modeling of two-way S-band Doppler to be accurate at the mHz level, close to its nominal accuracy at 10 s integration time. We analyze our ability to perform OD for GRAIL probes when using two different background lunar gravity fields, the GRAIL field GRGM900C (truncated to d/o 300) and the SELENE field SGM150J, along with different orbit parametrizations. We compare our orbits to the GNI1B positions provided as a by-product of GRAIL data processing at NASA/JPL. We get a significant improvement and orbit differences down to a few meters when using GRGM900C along with an appropriate parametrization of pulses and empirical accelerations. We noted that the orbit parametrization in terms of empirical accelerations and pseudo-stochastic pulses can be useful but has to be accurately chosen to avoid a degradation of the orbit. This is especially true when using a ”poorer” background gravity field. Based on the Doppler-only orbits, we perform orbit improvement in a combined Doppler and KBRR process. The two observation types are combined with $1 : 10^8$ weighting ratio to account for their relative accuracy. We get KBRR residuals down to the level of few μm/s even without an explicit model of non gravitational accelerations by using GRGM900C (up to d/o 300) and an appropriate parametrization. We finally evaluate the impact of KBRR on the absolute positioning of GRAIL-A and GRAIL-B by comparing them to the GNI1B positions. The orbits computed with a GRAIL gravity field and an appropriate parametrization are significantly improved. On the other hand, combined Doppler and KBRR orbit improvement based on pre-GRAIL fields proves to be difficult with our current setup and requires additional investigations. Possible improvements to our OD procedure include a more sophisticated constraining of the pseudo-stochastic pulses as well as the use of longer arcs to be adapted to the observations geometry and availability as well as to the desaturation maneuvers epochs [18].

6. References

[1] Pavlis, D. E., Wimert, J., and McCarthy, J. J. "GEODYN II system description." Tech. rep., SGT Inc., 2013. Contractor report, vols. 1-5.

[2] Moyer. Formulation for Observed and Computed Values of Deep Space Network Observables. Hoboken, NJ, 2003.

[3] GRGS Report. Algorithmic Documentation of the GINS Software, December 2013.

[4] Budnik, F., Morley, T. A., and MacKenzie, R. A. "ESOC's System for Interplanetary Orbit Determination: Implementation and Operational Experience." "18th International Symposium on Space Flight Dynamics," Vol. 548 of *ESA Special Publication*, p. 387. 2004.

[5] Dach, R., Beutler, G., Bock, H., Fridez, P., Gäde, A., Hugentobler, U., Jäggi, A., Meindl, M., Mervart, L., Prange, L., Schaer, S., Springer, T., Urschl, C., and Walser, P. Bernese GPS Software - Version 5.0. Astronomical Institute, University of Bern, 2007.

[6] Tapley, B. D., Bettadpur, S., Ries, J. C., Thompson, P. F., and Watkins, M. M. "GRACE Measurements of Mass Variability in the Earth System." Science, Vol. 305, pp. 503–506, Jul. 2004. doi:10.1126/science.1099192.

[7] Arnold, D., Bertone, S., Jäggi, A., Beutler, G., and Mervart, L. "GRAIL gravity field determination using the Celestial Mechanics Approach." Icarus, Vol. 261, pp. 182–192, Nov. 2015. doi:10.1016/j.icarus.2015.08.015.

[8] Zuber, M. T., Smith, D. E., Watkins, M. M., Asmar, S. W., Konopliv, A. S., Lemoine, F. G., Melosh, H. J., Neumann, G. A., Phillips, R. J., Solomon, S. C., Wieczorek, M. A., Williams, J. G., Goossens, S. J., Kruizinga, G., Mazarico, E., Park, R. S., and Yuan, D.-N. "Gravity Field of the Moon from the Gravity Recovery and Interior Laboratory (GRAIL) Mission." Science, Vol. 339, pp. 668–671, Feb. 2013. doi:10.1126/science.1231507.

[9] Konopliv, A. S., Park, R. S., Yuan, D.-N., Asmar, S. W., Watkins, M. M., Williams, J. G., Fahnestock, E., Kruizinga, G., Paik, M., Strekalov, D., Harvey, N., Smith, D. E., and Zuber, M. T. "High-resolution lunar gravity fields from the GRAIL Primary and Extended Missions." Geophysical Research Letters, Vol. 41, pp. 1452–1458, Mar. 2014. doi:10.1002/2013GL059066.

[10] Lemoine, F. G., Goossens, S., Sabaka, T. J., Nicholas, J. B., Mazarico, E., Rowlands, D. D., Loomis, B. D., Chinn, D. S., Neumann, G. A., Smith, D. E., and Zuber, M. T. "GRGM900C: A degree 900 lunar gravity model from GRAIL primary and extended mission data." Geophysical Research Letters, Vol. 41, pp. 3382–3389, May 2014. doi:10.1002/2014GL060027.

[11] Petit, G. and Luzum, B. e. "IERS Conventions (2010)." IERS Technical Note, Vol. 36, p. 1, 2010.

[12] Soffel, M., Klioner, S. A., Petit, G., Wolf, P., Kopeikin, S., et al. "The IAU 2000 resolutions for astrometry, celestial mechanics and metrology in the relativistic framework: Explanatory supplement." Astron.J., Vol. 126, pp. 2687–2706, 2003. doi:10.1086/378162.

[13] Jäggi, A., Hugentobler, U., and Beutler, G. "Pseudo-Stochastic Orbit Modeling Techniques for Low-Earth Orbiters." Journal of Geodesy, Vol. 80, pp. 47–60, 2006. doi:10.1007/s00190-006-0029-9.

[14] Jäggi, A., Beutler, G., Mervart, L., and Hugentobler, U. "Precise orbit determination for GRACE using GPS and K-band data." "37th COSPAR Scientific Assembly," 2008.

[15] Jäggi, A., Bock, H., Prange, L., Meyer, U., and Beutler, G. "GPS-only gravity field recovery with GOCE, CHAMP, and GRACE." Advances in Space Research, Vol. 47, pp. 1020–1028, Mar. 2011. doi:10.1016/j.asr.2010.11.008.

[16] Goossens, S., Matsumoto, K., and Ishihara, Y. "Improved High-Resolution Lunar Gravity Field Model From SELENE and Historical Tracking Data." "AGU Fall Meeting, Abstract P44B-05," 2011.

[17] http://pds geosciences.wustl.edu/. "PDS Geosciences Node.", 2014.

[18] Lemoine, F. G., Goossens, S., Sabaka, T. J., Nicholas, J. B., Mazarico, E., Rowlands, D. D., Loomis, B. D., Chinn, D. S., Caprette, D. S., Neumann, G. A., Smith, D. E., and Zuber, M. T. "High-degree gravity models from GRAIL primary mission data." Journal of Geophysical Research (Planets), Vol. 118, pp. 1676–1698, Aug. 2013. doi:10.1002/jgre.20118.